

LONGITUDINAL VARIATION OF LARGE SCALE VERTICAL  
MOTION IN THE TROPICS

by

ARTHUR C. KYLE  
B. A. , Texas A&M University (1965)  
B. S. , Pennsylvania State University ( 1966)

SUBMITTED IN PARTIAL FULFILLMENT OF THE  
REQUIREMENTS FOR THE DEGREE OF  
MASTER OF SCIENCE  
at the  
MASSACHUSETTS INSTITUTE OF TECHNOLOGY

January 15, 1970

Signature of Author.....  
Department of Meteorology, Jan. 1970

Certified by  
Thesis Supervisor

Accepted by.....  
Chairman, Departmental Committee on  
Graduate Studies

Lindgren

WITHDRAWN  
FROM  
MIT LIBRARIES  
MASS. INST. TECH.  
JAN 26 1970  
LIBRARIES

LONGITUDINAL VARIATION OF LARGE SCALE VERTICAL  
MOTION IN THE TROPICS

BY

ARTHUR C. KYLE

Submitted to the Department of Meteorology on 15 January 1970  
in partial fulfillment of the requirements for the degree  
of Master of Science.

ABSTRACT

Vertical motion is computed from the continuity equation from 40N to 30S for long term seasonal means. A three cell standing eddy structure was found in each season. The patterns are compared with rainfall climatology and satellite cloud data and found to show good agreement. The  $\bar{w}$  patterns for December 1962-February 1963 and December 1963-February 1964 are computed, and deviations in  $\bar{w}$  for each year from the long term mean for this season are compared with precipitation deviation from normal throughout the tropics, again with good results. The year to year change in  $\bar{w}$  is presented and discussed. It was found that the east-west gradient of vertical motion was much weaker in December 1963-February 1964. This is attributed to a change in phase of Walker's Southern Oscillation from positive to negative. This decrease in the east-west circulation was followed by an increase in the meridional Hadley cell circulation. This, coupled with an increase in the strength of the polar vortex, led to stronger mid-latitude westerlies during December 1963-February 1964.

Thesis Supervisor: Reginald E. Newell  
Title: Professor of Meteorology

TABLE OF CONTENTS

I. INTRODUCTION	5
II. DATA AND ANALYSIS	9
III. LONG TERM SEASONAL OMEGA	12
IV. COMPARISON OF DECEMBER 1962-FEBRUARY 1963 AND DECEMBER 1963-FEBRUARY 1964 WITH THE LONG TERM MEAN	17
V. COMPARISON BETWEEN DECEMBER 1962-FEBRUARY 1963 AND DECEMBER 1963-FEBRUARY 1964	21
VI. CONCLUSION	30

ACKNOWLEDGEMENTS

BIBLIOGRAPHY

LIST OF TABLES

Table 3.1 Zonal average of $\bar{w}$ ( $10^{-4}$ mb/sec) for the four seasons.	35
Table 4.1 Zonal average $\bar{w}$ ( $10^{-4}$ mb/sec) for December-February.	36
Table 4.2 Total precipitation (mm) and total deviation (mm) from 30 year normal for December 1962-February 1963 and December 1963-February 1964.	37
Table 5.1 Mean meridional velocity ( m/sec ) and momentum transport ( $m^2/sec^2$ ) by transient eddies for 200 mb.	44

LIST OF FIGURES

Figure 1.1	Mean sea-surface temperature for January ( $^{\circ}\text{C}$ ) (Hydrographic Office, U.S. Navy, 1944)	45
Figure 3.1	Mean vertical velocity at 500 mb for December- February. Units: $10^{-4}$ mb/sec.	46
Figure 3.2	Mean vertical velocity at 500 mb for March-May. Units: $10^{-4}$ mb/sec.	47
Figure 3.3	Mean vertical velocity at 500 mb for June-August. Units: $10^{-4}$ mb/sec.	48
Figure 3.4	Mean vertical velocity at 500 mb for September- November. Units: $10^{-4}$ mb/sec.	49
Figure 4.1	Mean vertical velocity at 500 mb for December 1962-February 1963. Units: $10^{-4}$ mb/sec.	50
Figure 4.2	Mean vertical velocity at 500 mb for December 1963-February 1964. Units: $10^{-4}$ mb/sec.	51
Figure 4.3	Deviation of mean vertical velocity at 500 mb for December 1962-February 1963 from the long term mean for December-February. Units: $10^{-4}$ mb/sec.	52
Figure 4.4	Deviation of mean vertical velocity at 500 mb for December 1963-February 1964 from the long term mean for December-February. Units: $10^{-4}$ mb/sec.	53
Figure 4.5	Total deviation of precipitation for December 1962- February 1963 from the 30 year mean. Units: mm.	54
Figure 4.6	Total deviation of precipitation for December 1963- February 1964 from the 30 year mean. Units: mm.	55
Figure 5.1	Change in mean vertical velocity from December 1962-February 1963 to December 1963-February 1964. Units: $10^{-4}$ mb/sec.	56

## I. INTRODUCTION

It has long been thought that air-sea interaction plays an important part in the general circulation of the atmosphere. The sea-surface temperature depends on the wind field, and a change in one will bring about a change in the other. Therefore, it is of particular interest to look at a case of a significant departure from normal of sea-surface temperature over a large area.

A map of sea-surface temperatures for the equatorial South Pacific (Fig. 1.1) shows that the water from about 160W to the South American coast is colder than the global average for these latitudes and that the Pacific waters west of 160W are warmer than the global average. The air above the cold water belt is too cold and heavy to join in the ascending motion in the Hadley circulation. Instead, the equatorial air flows westward to the warm west Pacific where it can take part in large-scale moist-adiabatic ascent (Bjerknes, 1969). There is then a return flow toward the east in the upper troposphere or lower stratosphere and accompanying descent in the eastern Pacific. Thus there should be large-scale cloudiness over areas of warm water and relatively clear skies over areas of cold water. This can be easily seen on maps of global cloudiness obtained by satellite observations (Hubert et al., 1969).

Bjerknes (1969) calls this exchange of air between eastern and western hemispheres the "Walker Circulation". This is a part of the mechanism of the "Southern Oscillation" statistically defined by Sir Gilbert Walker and Walker and Bliss in the World Weather I to VI sequence of research reports (referenced in the Bjerknes article). Troup (1965) discusses the Southern Oscillation and also suggests that changes in the direct toroidal circulation between the warmer eastern and cooler western hemispheres have a major effect on the Southern Oscillation.

The westward extent of the cold water of the South Equatorial Current depends on upwelling of colder water from below, which depends on the distribution and strength of the easterlies along the Equator. Bjerknes (1969) presents a time series of sea and air temperature from 1950 to 1967 for Canton Island ( $02^{\circ} 48'S$ ,  $171^{\circ} 43'W$ ). Most of the time water of equatorial upwelling reaches Canton Island, but in three cases (late 1957, late 1963 and late 1965) the sea-surface temperature is warmer than the air temperature. These periods are also marked by above average precipitation. Krueger and Gray (1969) show these same data in a time series as well as showing that the easterly component of the surface wind approaches zero during these periods. In addition, Krueger and Gray show maps of December-February seasonally averaged sea-surface temperature anomalies for the eastern tro-

pical Pacific for the five year period 1962 to 1967. These maps show that Canton Island is fairly representative of most of the equatorial Pacific in that the whole area from  $180^{\circ}$  to South America was abnormally warm during December 1963 - February 1964 and December 1965 - February 1966. Bjerknes concludes that during these periods, the large-scale ascending air cell has moved eastward to include Canton Island. Support for this hypothesis is shown by satellite nephanalyses (Bjerknes et al., 1969). The position of the  $\frac{6}{10}$  isoneph at the Equator moves eastward as the sea-surface temperature decreases. Bjerknes et al., (1969) present monthly mean cloud nephanalyses (taken from Godshall et al., 1969) for several periods, showing that on the average there is little cloudiness from the Equator to  $10^{\circ}\text{S}$  east of  $180^{\circ}$  except during those months when the warm water has moved eastward.

Because these periods of anomalously warm water at Canton Island are accompanied by increases in precipitation, they are periods of greater release of latent heat. The Hadley circulation, which is primarily driven by the release of latent heat in its ascending branch, is thus, accelerated to produce a greater transport of heat and momentum to higher latitudes. This is then shown (Bjerknes, 1966, 1969) to maintain stronger than normal westerlies in the middle latitudes.



The purpose of this paper is to examine large-scale vertical motion patterns in the tropics by computing  $\omega \left( \frac{\partial p}{\partial t} \right)$ . First, the long term seasonal means are looked at and related to the observed precipitation patterns. Next,  $\bar{\omega}$  is computed for December 1962-February 1963, a period of near normal sea-surface temperature at Canton Island, and for December 1963-February 1964, a period of above normal sea-surface temperature for the eastern equatorial Pacific. Each period is compared with the long term mean. Finally, the change from one year to the next is investigated with special interest in the relationship between vertical motion and sea-surface temperature in the eastern equatorial Pacific. Also of interest is the relationship between changes in the Hadley cell circulation and the circulation at higher latitudes.

## II. DATA AND ANALYSIS

The data used in this paper were originally put in working form by J. W. Kidson and a detailed explanation of the data and its sources can be found in Chapter 2 of Newell et al., (1970). The data are from 303 radiosonde and radar wind stations within the overall period July 1957 to December 1964. All available stations between latitudes 35N and 30S were used and some additional stations were used to extend the area covered to 45N. Many stations did not report regularly throughout the entire period, so the quantity and quality of the data varied considerably between stations. Most data were taken at 0000 GMT, but 0600 GMT and 1200 GMT data were included where necessary. A complete station list along with the source and reporting period is presented in Newell et al., (1970).

The daily data for each station were first used to compute monthly mean statistics at all available levels from the surface to 7 mb including the quantities  $\bar{u}$ ,  $\bar{v}$  and  $\overline{u'v'}$  used here. The long term means for four seasons, December-February, March-May, June-August and September-November were computed, using the seven years of data. Maps of the long term means for the quantities  $\bar{u}$ ,  $\bar{v}$  and  $\overline{u'v'}$  can be found in Chapter 3 of Newell et al., (1970).

The continuity equation

$$\frac{\partial \omega}{\partial p} = - \nabla \cdot V$$

is used to obtain  $\omega$ , the vertical velocity in pressure coordinates. It is assumed that  $\omega=0$  at 1000 mb as was done for example by Lateef (1967). Since the vertical velocities thus computed tend to increase with height, the result is a non-zero value for the net divergence in a column. In this study  $\omega$  at 100 mb was set to zero and the  $\omega$  at each lower level was reduced proportionately.

i. e. 
$$\omega'(p) = \omega(p) - \left[ \frac{1000-p}{900} \right] \omega(100)$$

The grid used was 20 degrees of longitude and 10 degrees of latitude. The vertical velocity was computed at the center of the grid using the three monthly means of  $\bar{u}$  and  $\bar{v}$  as read from the respective maps at the significant levels from 1000 mb to 100 mb. Whereas  $\omega$  was computed for each level, it was decided that the value at 500 mb would be the best to be used to compare with rainfall.

In order to study the difference in the vertical motion patterns from year to year, the December-February season for 1963 and 1964 was chosen. The zonal and meridional wind components were averaged to give a three month mean for each station reporting during December 1962-February 1963. These were then plotted and hand analyzed for each significant level from 1000 mb to

100 mb. The December 1963-February 1964 season was chosen because during this time the sea-surface temperature at Canton Island was abnormally warm. Thus, one purpose of this paper is to investigate the "Walker Circulation" (Bjerknes, 1969). It was found that most of the station wind data north of 30N had been obtained from the five years of data under the Northern Hemisphere General Circulation Study of Professor V.P. Starr, and this data ended in April 1963. Therefore, the analysis region was reduced to 30N for December 1963-February 1964. The  $\bar{u}$  and  $\bar{v}$  maps for these two periods are in Chapter 10 of Newell et al., (1970). Whereas there were 260 stations available for December 1962-February 1963, there were only 110 stations for December 1963-February 1964. Since nearly all the stations for which data were not available for the second period were north of 30N, it was not thought that this would greatly influence the equatorial regions which are of primary concern in this paper. The  $\bar{w}$  map for December 1962-February 1963 was computed from 35N to 25S as were the seasonal long term  $\bar{w}$  maps. The  $\bar{w}$  map for December 1963-February 1964 covers 25N to 25S.

### III. LONG TERM SEASONAL OMEGA

In this chapter the long term means of  $\bar{\omega}$  for the seasons December-February, March-May, June-August and September-November are presented. To check on the accuracy of these maps, computed as outlined in Chapter 2, they are compared with rainfall climatology and with satellite cloud nephanalyses. Because of the scarcity of wind reporting stations in all but the continent sections of the tropics and because of the large grid used in the computation of  $\bar{\omega}$ , it is not assumed that the numerical values shown on these  $\bar{\omega}$  maps are entirely correct. However, it is thought that the patterns fit well with what is to be expected for vertical motion and that the numbers can be compared relative to each other.

The long term seasonal  $\bar{\omega}$  maps are presented in Figs. 3.1-3.4. The units are  $10^{-4}$  mb/sec ( $\approx 1.5$  mm/sec). Easily seen is the Intertropical Convergence Zone (ITCZ) and its movement throughout the year. To further show this, zonal averages for  $\bar{\omega}$  are computed for each season in Table 3.1. In the December-February season, the ITCZ is slightly south of the equator in all regions. In June-August the ITCZ has moved north of the equator, to about 5N north over South America and Africa. There is widespread ascent in the monsoon regions of Southeast Asia and

the western Pacific, with the centers of ascent at 10N. For both the March-May season and the September-November season the ITCZ is found north of the equator, being somewhat further north during September-November. It is also noted that the Hadley cell is a little stronger in June-August than in December-February. Kidson et al., (1969) found that the mass circulation of the northern winter cell is approximately  $1.7 \times 10^{14}$  g/sec and that the southern winter cell is about  $2.0 \times 10^{14}$  g/sec.

Perhaps the most interesting result of this study was the finding of the three cell structure of vertical motion in the equatorial regions. For each season there are three main areas of upward motion: over South America, over Africa, and a broad area of ascent with centers near Indonesia and in the western Pacific. There are areas of descending air between the areas of rising air or in some cases a large decrease in the magnitude of the upward motion. In the past most studies of the Hadley circulation have used zonal averages, and this three cell pattern is hidden by the averaging. Recent satellite cloud picture studies have shown alternating clear and cloudy regions in the tropics, and Hubert et al., (1969) have suggested that there is an east-west gradient of vertical motion. Troup (1965) and Bjerknes (1969) show how a toroidal circulation exists between the hemispheres in the Pacific.

It is assumed that part of the air that rises in these three cells is carried zonally as well as meridionally. This study seems to confirm that hypothesis.

The upward cell over South America is markedly constant in longitude throughout the year. The center is along 70W for each season, moving only north and south with the sun. It is strongest during December-February when it is furthest south. The large area of ascent in the western Pacific and near Indonesia has little variation with longitude also. One center is generally near 95-100E and the other remains on 170E. Whereas the center over South America was weakest in June-August, both centers in the western Pacific are strongest in this season.

The area of rising motion over Africa varies the most longitudinally. The center goes from about 30E in December-February to 10E in June-August. It is this region which can best be compared with rainfall climatology, using the mean monthly rainfall maps for Africa as compiled by Thompson (1965). For December-February, Thompson shows the area of maximum rainfall to be 300-400 mm per month at about 13S and 30E, a little south of the area of maximum ascent on Fig. 3.1. From March to April, the rainfall area moves to north of the equator, being centered on the equator in April with the maximum (200-300 mm per month) nearer the western coast. This agrees well with Fig. 3.2. During

June-August the maximum rainfall area has moved almost entirely north of the equator, becoming centered at 5N. There are two centers of heavy precipitation, the coast of Nigeria with about 400-600 mm per month and along the coast of Sierra Leone, Liberia and Ivory Coast with a maximum of 1000 mm in Sierra Leone in August. Fig. 3.3 shows the center over Nigeria but not the western one. From September to November, the maximum rainfall area moves southward along the western coast of Africa to become centered over Gabon in November. The three monthly average would show the center of the rainfall belt to be slightly north of the equator and mainly in the western half of the continent with 400-600 mm per month. This is in good agreement with Fig. 3.4. It is also noted that the March-May season has the least monthly precipitation and the weakest rising motion and that the June-August season has the greatest monthly precipitation and the strongest rising motion. The areas of subsidence on Figs. 3.1-3.4 also correspond well with areas of Africa which Thompson shows as having very little rain. In particular, the continent north of the equator is dry during December-February and south of the equator is dry during June-August. The satellite nephanalyses of monthly cloudiness of Kornfield and Hasler (1969) show the same thing.

Figs. 3.1-3.4 show several interesting features recently seen in analyses of satellite cloud brightness data. A band of



cloudiness maximum is oriented southeast to northwest in the southwestern Pacific from about 30S and 150W to the equator. It intersects the equator at different longitudes, depending on the westward extent of the upwelling of the South Equatorial Current (Bjerknes et al., 1969). Corresponding with this cloudiness band is the southeastward extension of ascent from New Guinea to 30S and 150W on Figs. 3.1 and 3.2. There is downward motion in June-August (Fig. 3.3) in this region, and Hubert et al., (1969) show that the cloudiness band is less defined in this season. A southeastward extension of cloudiness from South America shown by Hubert et al., (1969) is not evident in Figs. 3.1-3.4, except possibly in December-February.

The  $\bar{\omega}$  maps computed in this study also would not support the theory of a double ITCZ for most areas. It is only in June-August that there is a continuous belt of ascent through the Atlantic and Indian Oceans, and even then it is narrow and weak. There is subsidence in the eastern Pacific extending generally to 20S in all seasons, with only a weak ascent belt stretching from South America to 130W in the Northern Hemisphere in summer. The satellite cloud pictures of Hubert et al., (1969) show two cloud bands exist over the western Pacific during three seasons. This cannot be seen on Figs. 3.1-3.4 due to the great distance between wind reporting stations in this area and in part to the grid size used

in the computation of  $\bar{\omega}$ .

#### IV. COMPARISON OF DECEMBER 1962-FEBRUARY 1963 AND DECEMBER 1963-FEBRUARY 1964 WITH THE LONG TERM MEAN

Based on the evidence presented in Chapter 3, it appears that the maps computed in this study present a true picture of the large scale vertical motions in the tropics. In this chapter, this technique is used to look at  $\bar{\omega}$  for two particular December-February seasons and their differences from the long term  $\bar{\omega}$  for December-February.

Figs. 4.1 and 4.2 are the December 1962-February 1963 and December 1963-February 1964 maps for  $\bar{\omega}$  at 500 mb. The units are the same as used for the long term seasonal means in Chapter 3. It was assumed at the beginning that December 1962-February 1963 was an "average" year, and the major features are the same as on the long term  $\bar{\omega}$  maps for this season (Fig. 3.1). There is a shift in the position of some centers of vertical motion. The descent area in the eastern Pacific has pushed further southward and the descent areas in the Atlantic have strengthened as did the area in the western North Pacific. There are increases in ascent along the western coast of Mexico and the center over South America. The center over southern Africa is situated southward

and is stronger. These and other changes can be seen in Fig. 4.3, a difference map found by graphically subtracting the long term  $\bar{\omega}$  for December-February from  $\bar{\omega}$  for December 1962-February 1963 (Fig. 4.1 minus Fig. 3.1). December 1963-February 1964 was a season of abnormally warm sea-surface temperature in the equatorial regions of the eastern Pacific. Therefore, it is of particular interest to see what effect this has on the  $\bar{\omega}$  pattern for this three month period (Fig. 4.2). There are several significant differences between  $\bar{\omega}$  for December 1963-February 1964 and the long term mean (Fig. 3.1). The descent in the warm water region of the eastern Pacific is weaker. Also there is a large shift to the southeast by the center of the ascent region over South America and the center over Africa. The Gulf of Mexico and Caribbean waters have become a region of strong descent and China has become a region of strong ascent. These changes are presented in the difference map Fig. 4.4 (Fig. 4.2 minus Fig. 3.1).

Table 4.1 is zonal averages of  $\bar{\omega}$  for the three periods under investigation. The latitude of maximum ascent is 5S for all periods, with the long term mean being the greatest. It is noted that the rising branch of the Hadley cell for December 1963-February 1964 is stronger than for the preceding year at all latitude circles except 5N, and is appreciably stronger at 10S and 15S. This reflects the southeastward shift of the maximums over South America

and Africa and the decreases in the subsidence cells in the oceans at these latitudes for this year.

As a check on the differences from normal of the  $\bar{w}$  maps for these two December-February seasons, monthly precipitation records for stations in the tropics were looked at. Table 4.2 is a list of the three monthly total of precipitation and the three monthly total deviation from the 30 year normal for as many stations as could be found for December 1962-February 1963 and December 1963-February 1964. The deviations were then plotted for each station and the shaded areas on Figs. 4.5 and 4.6 represent greater than normal precipitation. The solid lines were drawn where there was sufficient data coverage to justify this being done. The clear areas represent below normal precipitation or lack of data. Therefore, Fig. 4.5 may be compared directly with Fig. 4.3 which shows the difference between  $\bar{w}$  for December 1962-February 1963 and the long term mean. Negative areas on Fig. 4.3 indicate an increase in upward motion which should correlate well with the shaded areas on Fig. 4.5. In general there is good agreement between Fig. 4.3 and Fig. 4.5. The increased ascent regions are South America below the equator, almost all of Africa, Indonesia and western Australia, and the western Pacific from the equator to 20N. All of these areas received above aver-

age rainfall during this period. The major areas which had an increase in descent were Southeast Asia and the Philippines and the eastern Pacific west of 150W. The same comparison can be made between Fig. 4.4 and Fig. 4.6 (December 1963-February 1964). Here the regions with an increase in upward motion are the southern half of South America, northwestern and southeastern Africa, Southeast Asia, and the islands in the equatorial western Pacific. For the most part, these regions were wetter than normal. The northern half of South America, central Africa, and Australia received less than normal precipitation. It can be seen in Table 4.2 that some stations had significantly large departures from normal, and that all of these were in agreement with the  $\bar{w}$  departure maps.

V. COMPARISON BETWEEN DECEMBER 1962-FEBRUARY  
1963 AND DECEMBER 1963-FEBRUARY 1964

In the preceding chapter it was shown how the  $\bar{w}$  pattern for December 1962-February 1963 and December 1963-February 1964 differed from the pattern for the long term mean for this season. In this chapter the  $\bar{w}$  difference between the two years is looked at. The Southern Oscillation is examined in an attempt to find a cause for the change. The relation between this change in the ascending branch of the Hadley cell and the circulation at higher latitudes is also looked at.

In previous studies of changes of the circulation in the eastern Pacific (Bjerknes, 1969, Kruger and Gray, 1969), it was shown that when the sea-surface temperature at Canton Island becomes abnormally warm, there is an increase in cloudiness and rainfall, and a decrease in the strength of the easterlies. Bjerknes (1969) concluded that this is caused by an easterly shift in the ascending branch of the "Walker Circulation", a toroidal circulation between the eastern Pacific (cold water and persistent high pressure) and the western Pacific (warm water and low pressure). In a time sequence graph Bjerknes shows that significantly above normal precipitation at Canton

Island occurs only with the warm sea-surface temperature anomaly. It can be seen in Table 4.2 that this is true for the warm water period of December 1963-February 1964 at Canton Island. Also an eastward shift by the ascent region of the western Pacific can be seen on Figs. 4.1 and 4.2, where the  $\bar{\omega} = 0$  line has moved about 8 degrees to include Canton Island in the second year.

Looking once again at Fig. 4.1, we find that for December 1962-February 1963, the centers of upward motion and the centers of downward motion are stronger than for the long term mean (Fig. 3.1). The change in  $\bar{\omega}$  from December 1962-February 1963 to December 1963-February 1964 shows there are some interesting differences throughout the equatorial regions. This is shown in Fig. 5.1 (Fig. 4.2 minus Fig. 4.1). Here the negative areas show an increase in upward motion or a decrease in downward motion for the second year, depending on the region in which the change takes place. It is noted that for the second year, the centers of ascent (South America, Africa, Indonesia) are weaker and the centers of descent (eastern Pacific, Atlantic and Indian Oceans) are weaker also. In other words, the east-west gradient of vertical motion, which was stronger than normal in December 1962-February 1963, is greatly diminished in December 1963-February 1964. Therefore

it appears that the "Walker Circulation" has been decreased in strength in this year. It also appears that there is an east-west "Walker" type of circulation between South America and the Atlantic Ocean and between Africa and the Indian Ocean as well.

The 1000 mb  $\bar{u}$  maps (Chapter 10, Newell et al., 1970) for these two years show that the equatorial easterlies in all three oceans were weaker in December 1963-February 1964.

It is the strength of the southeast Pacific anticyclone which affects the strength of the equatorial Pacific easterlies (Troup, 1965). The pressure variations of this anticyclone are influenced by Walker's Southern Oscillation, which shows a strong negative correlation between pressure anomalies in the southeast Pacific and the tropical Indian Ocean. Easter Island (29S, 109W) appears to be the center of the eastern Pacific pressure anomaly and Djakarta the center of the Indian Ocean pressure anomaly. A positive phase of the Southern Oscillation means above normal pressure at Easter Island and below normal pressure at Djakarta. This leads to a strong "Walker Circulation" between the eastern and western hemispheres. Therefore it appears that a change of phase of the Southern Oscillation could cause such a change as occurred in the "Walker Circulation" from December 1962-February 1963 to December 1963-February 1964.



The author was unable to obtain any of Walker's original papers, but he did find an excellent review of Walker's work (including numerous figures and tables) by Montgomery (1939). It was not possible to compute the Southern Oscillation Index for the two years in question, but it was found that Canton Island, which Walker shows to be positively correlated with the Southern Oscillation, had a pressure deviation of +1.2 mb in December 1962-February 1963 and a pressure deviation of -0.8 mb in December 1963-February 1964. Djakarta had a pressure deviation of -0.6 mb and +0.3 mb for these two periods, respectively. Walker also has a correlation between the Southern Oscillation in December-February and precipitation for the same season. This shows that Canton Island precipitation deviation is negatively correlated and Djakarta precipitation deviation positively correlated with the Southern Oscillation. Table 4.2 shows this is consistent for the two stations. Other areas with precipitation positively correlated with the Southern Oscillation in December-February are South America north of 20S, central Africa, and northern Australia and the islands in the western Pacific near Yap. These areas all had above average precipitation in December 1962-February 1963 and below average precipitation the year later (Fig. 4.5 and Fig. 4.6). Therefore it was concluded that

the Southern Oscillation was positive during December 1962-February 1963 and was negative the following year. Since positive sea-surface temperature anomalies in the equatorial eastern Pacific occur when the "Walker Circulation" is weak, this must mean that they occur when there is a change from a positive to a negative phase of the Southern Oscillation.

Krueger and Gray (1969) show three periods of abnormally warm water at Canton Island: April 1957-May 1958, June 1963-March 1964, and June 1965-May 1966. Bjerknes (1969) has carefully analyzed the various parameters during 1963. He found that from March to April there was a pressure drop at Easter Island. This decrease in the southeast Pacific anticyclone was followed one month later by an increase in sea-surface temperature at 165W along the equator. In June the pressure at Djakarta rose nearly 2 mb. Thus was the pressure gradient for the "Walker Circulation" reduced during 1963. Troup (1965) says that the changes in phase of the Southern Oscillation occur mainly in late southern autumn or early winter. Walker found a correlation of +0.84 between the Southern Oscillation in June-August and the Southern Oscillation in the following December-February (Montgomery, 1939). Thus, it appears that the change in phase of the Southern Oscillation which occurred during the se-

cond quarter of 1963 could explain the change in the vertical motion pattern in December 1963-February 1964.

The effect that the change in the east-west gradient of vertical motion has on the zonal average of  $\bar{w}$  can be seen in Table 4.2. As was pointed out in Chapter 4, the ascending branch of the Hadley is stronger in December 1963-February 1964 than in the previous year. This should be followed by a greater export of angular momentum from the equatorial regions. Kidson et al (1969) show that the region of strongest divergence of total momentum is near 200 mb and about 10 degrees of latitude in the winter hemisphere, and that most of the transport is contributed by the transient eddies. The zonal average for  $\bar{v}$  and the transient eddies for the two northern winter seasons is shown in Table 5.1. It is noted that the momentum transport by the transient eddies into both hemispheres occurs at about 15N, and the larger transport occurs in December 1963-February 1964. This larger momentum transport would contribute to stronger westerlies at higher latitudes, as was shown by Bjercknes (1969). Krueger and Gray (1969) show that there was a larger transformation from eddy to zonal kinetic energy in the Northern Hemisphere north of 20N during the 1963-64 autumn and winter.

Walker devised North Atlantic and North Pacific Oscillations in addition to his Southern Oscillation (Montgomery, 1939). He found that there was a high positive correlation between pressure in the 20N to 50N belt and both oscillations, and a high negative correlation between pressure poleward of 50N and both oscillations. When the North Atlantic Oscillation is positive, there is a decrease in pressure in the polar regions and an increase in pressure in the subtropical regions, which leads to an increase in the general circulation over the Atlantic Ocean. There is not only an increase in the north-south pressure gradient, but a poleward displacement of the Icelandic Low and the Azores High. The North Pacific Oscillation has much the same effect in that ocean. In relating these oscillations to the Southern Oscillation, Walker found the North Pacific Oscillation in December-February has coefficients of  $-0.52$  with the Southern Oscillation both in the same quarter and in the June-August before. Therefore we find a linkage between the east-west pressure gradient (Southern Oscillation) and the north-south pressure gradient (two northern oscillations) and their related circulations. When the Southern Oscillation is positive, the east-west "Walker" type circulation is strong. When the Southern Oscillation changes to the negative, usually in June-August, the North Atlantic and North Pacific Oscillations are positive six months later. Thus, when the

east-west circulation is weak the north-south circulation is strong. The author concludes that this happened in December 1963-February 1964. The pressure change from January 1963 to January 1964 (Bjerknes, 1969) indicates a strengthening of the Aleutian Low and the subtropical Pacific High, showing an increase in the north-south pressure gradient after the decrease in the east-west pressure gradient which occurred in March-July of 1963. In Fig. 5.1 we see a decrease in the east-west gradient of vertical motion in December 1963-February 1964, and in Table 4.1 we see an increase in the north-south gradient of vertical motion for this season. The author concludes that it is a combination of the two which leads to the increase in westerlies in December 1963-February 1964.

Since it appears that a change in phase of the Southern Oscillation has a pronounced effect on the circulation both in the tropics and at higher latitudes, it is important to find a cause for the change. Several explanations have been offered. Troup (1965) found no periodicity for the Southern Oscillation. He concluded that since the change is most likely in southern winter, variations in cyclonic activity in the southeast Pacific could initiate a change in the anticyclone of that region. Professor H. C. Willett (personal communication) has pointed out that since June-August is the monsoon season in Asia, a change in the monsoon

circulation could be reflected through the Southern Oscillation to the Southeast Pacific anticyclone. Schell (1956) says that the strength of the Southeast Pacific anticyclone depends on the outflow of subantarctic water along the west coast of South America. Therefore, a variation in corpuscular radiation acting on the Antarctic circulation could influence the strength and extent of the cold ocean current. The physics involved in this is not clear.

It is not possible from the present study to conclude which of the above is the source of change of the Southern Oscillation, as they all could be a factor. A close look at the circulation in the equatorial regions during the second and third quarter of 1963 might help in solving this intriguing question.

## VI. CONCLUSION

From the results presented in this paper, it appears that the method of computing vertical motion from the equation of continuity is indeed valid. While there are large areas in the tropics with very few reporting stations, the data are adequate to reveal the large scale circulation. Good agreement was found between the computed  $\bar{w}$  patterns and rainfall and satellite cloud data.

The results of this study offer support for an east-west toroidal circulation between the major areas of ascent and descent in the equatorial regions. It appears that the strength of this circulation depends on the phase of Walker's Southern Oscillation, the circulation being stronger when the Southern Oscillation is positive. The changes in sea-surface temperature and precipitation patterns that took place in the equatorial Pacific during 1963 are attributed to a change of phase of the Southern Oscillation. The change in the general circulation at higher latitudes which was found to follow the Southern Oscillation change makes it necessary to monitor the Southern Oscillation, perhaps in the abbreviated form of Willett and Bodurtha (1952), as an aid to long range forecasting.

There is still some question as to the role of sea-surface temperature in the general circulation of the atmosphere (Bjerknes, 1969). This author agrees with the results of Helland-Hansen and Nansen (reviewed by Montgomery, 1939) that water and air temperature anomalies result from anomalies in the local winds. It is evident that more research in the area of air-sea interaction is necessary.



### ACKNOWLEDGEMENTS

The author is grateful to the United States Air Force who sponsored his work at MIT through the Air Force Institute of Technology. This study developed from a suggestion by Professor Reginald E. Newell, and the author is forever thankful to him for his continued guidance and encouragement. Thanks are also due to Miss Isabelle Kole for drawing the figures and to Miss Kora Gordon for typing the manuscript.

BIBLIOGRAPHY

- Bjerknes, J., 1966: A possible response of the atmospheric Hadley circulation to equatorial anomalies of ocean temperature. Tellus, 18, pp. 820-829.
- Bjerknes, J., 1969: Atmospheric teleconnections from the equatorial Pacific. Mon. Wea. Rev., 97, pp. 163-172.
- Bjerknes, J., L. J. Allison, E. R. Kreins, F. A. Godshall and G. Warnecke, 1969: Satellite mapping of the Pacific tropical cloudiness. Bull. Amer. Meteor. Soc., 50 pp. 313-322.
- Godshall, F. A., L. J. Allison, E. R. Kreins and G. Warnecke, 1969: An atlas of average cloud cover over the tropical Pacific Ocean, Part II of examples of the usefulness of satellite data in general circulation research. NASA Technical Note, Goddard Space Flight Center, Greenbelt, Md.
- Hubert, L. F., A. F. Krueger and J. S. Winston, 1969: The double Intertropical Convergence Zone - fact or fiction? J. Atmos. Sci., 26, pp. 771-773.
- Hydrographic Office, U. S. Navy, 1944: World atlas of sea surface temperatures. 2nd Edition, H. O. Pub. No. 225, 1954 reprint. pp 49.
- Kidson, J. W., D. G. Vincent and R. E. Newell, 1969: Observational studies of the general circulation of the tropics: long term mean values. Q. J. Roy. Meteor. Soc., 95, pp. 258-287.
- Kornfield, J. and A. F. Hasler, 1969: A photographic summary of the earth's cloud cover for the year 1967. J. App. Meteor., 8, pp. 687-700.
- Krueger, A. F., and T. I. Gray, 1969: Long-term variations in equatorial circulation and rainfall. Mon. Wea. Rev., 97, pp. 700-711.

- Lateef, M.A., 1967: Vertical motion, divergence, and vorticity in the troposphere over the Caribbean, August 3-5, 1963. Mon. Wea. Rev., 95, pp. 778-790.
- Montgomery, R.B., 1939: Report on work of G.T. Walker. Mon. Wea. Rev., Supp. 39, pp. 1-22.
- Montgomery, R.B., 1939: Discussion of some theories on temperature variations in the North Atlantic Ocean and the atmosphere. Mon. Wea. Rev., Supp. 39, pp. 52-57.
- Newell, R.E., J.W. Kidson and D.G. Vincent, 1970: The general circulation of the tropical atmosphere and interactions with extra-tropical latitudes. (To be published by M.I.T. Press).
- Schell, I.I., 1956: On the nature and origin of the Southern Oscillation. J. Meteor., 13, pp. 592-598.
- Thompson, B.W., 1965: The Climate of Africa. Oxford University Press, Nairobi, pp. 132.
- U.S. Department of Commerce- Weather Bureau: Monthly Climatic Data for the World. December 1962, January, February, December, 1963, January, February 1964.
- Willett, H.C. and F.T. Bodurtha, 1952: An abbreviated Southern Oscillation. Bull. Amer. Meteor. Soc., 33, pp. 429-430.

TABLE 3.1

Zonal Average of  $\bar{\omega}$  ( $10^{-4}$  mb/sec) For The Four Seasons

	$[\bar{\omega}]$	$[\bar{\omega}]$	$[\bar{\omega}]$	$[\bar{\omega}]$
	Dec-Feb	Mar-May	Jun-Aug	Sep-Nov
25N	3.32	1.97	-0.97	-0.03
15N	5.43	4.12	-2.23	-1.01
05N	-0.52	-3.14	-5.82	-3.38
EQ	-3.16	-3.57	-2.28	-2.28
05S	-5.40	-2.82	0.83	-0.59
15S	-1.87	1.37	5.90	4.49
25S	0.48	2.30	6.14	3.06

TABLE 4.1

Zonal Average  $\bar{w}$  ( $10^{-4}$  mb/sec) For December-February

	$[\bar{w}]$ long term	$[\bar{w}]$ 62-63	$[\bar{w}]$ 63-64
25N	3.32	5.44	4.05
15N	5.43	2.32	2.07
05N	-0.52	-0.92	-0.70
EQ	-3.16	-2.36	-3.07
5S	-5.40	-3.68	-4.34
10S	-3.56	-3.07	-4.11
15S	-1.87	-1.65	-3.09
25S	0.48	0.51	0.27

TABLE 4.2 TOTAL PRECIPITATION (MM) AND TOTAL DEVIATION (MM) FROM 30 YEAR NORMAL FOR DECEMBER 1962-FEBRUARY 1963 AND DECEMBER 1963-FEBRUARY 1964

STATION	LAT	LONG	TOTAL DEV DEC62-FEB63	TOTAL DEV DEC63-FEB64
UNITED STATES				
SAN DIEGO	32 44N	117 10W	40 -118	45 -113
PHOENIX	33 26N	112 01W	55 -8	6 -57
EL PASO	31 48N	106 24W	24 -10	1 -34
SAN ANTONIO	29 32N	98 28W	156 +26	158 +28
BROWNSVILLE	25 55N	97 28W	70 -46	113 -3
LITTLE ROCK	34 44N	92 14W	133 -204	161 -176
SHREVEPORT	32 2 N	3 49W	15 -1 4	211 -1 0
NEW ORLEANS	29 59N	90 15W	396 +93	513 +210
CHARLESTON	32 54N	80 02W	241 +20	418 +187
JACKSONVILLE	30 25N	81 39W	387 +181	442 +250
MIAMI	25 49N	80 17W	110 -31	175 +34
NASSAU	25 03N	77 28W	92 -26	240 +122
MEXICO				
MAZATLAN	23 11N	106 26W	6 -41	
TAMPICO	22 13N	97 51W	41 -46	140 +63
MORELIA	19 42N	101 07W	11 -17	
VERACRUZ	19 12N	96 08W	41 -23	
ACAPULCO	16 50N	99 55W	20 +2	
CENT AMER AND ISLANDS				
PUERTO PLATA	19 41N	70 40W	413 -265	959 +281
SANTO DOMINGO	18 27N	69 53W	258 +99	147 -12
SAN PEDRO SULA	15 30N	88 01W	90 -137	
CATAMAS	14 54N	85 55W	90 +1	50 -39
SAN SALVADOR	13 43N	89 12W	60 +45	1 -15
SWAN ISLAND	17 24N	83 56W	111 -151	123 -136
SAN JUAN ISLA VERDE	18 26N	66 00W	219 -112	111 -220
KINGSTON	17 56N	76 47W	90 +27	90 +27
RAIZET	16 16N	61 31W	170 -130	170 -130
FORT-DE-FRANCE	14 37N	61 04W	340 +72	200 -90
DR A PLESMAN APT	12 11N	68 59W	120 -73	39 -159
PIARCO APT	10 37N	61 21W	200 -91	170 -121
VENEZUELA				
MARACAIBO	10 39N	71 36W	40 +30	1 -9
BARCELONA	10 07N	64 41W	61 +28	10 -23
CIUDAD BOLIVAR	08 09N	63 33W	56 -33	30 -59
FR GUIANA				
CAYENNE	04 50N	52 22W	1640 +469	490 -681
SANT ELENA	04 36N	61 07W	224 -53	90 -187
EQUADOR				
QUITO	00 08S	78 29W	300 -54	160 -194
QUAYAQUIL	02 10S	79 50W	303 -226	380 -149
BRAZIL				
UAUPES	00 08S	67 05W	800 +30	
BELEM	01 28S	48 29W	630 -292	780 -142
QUIXERAMBOIM	05 12S	39 18W	350 +154	460 +226
PORT VELHO	08 46S	63 55W	910 -67	740 -237
REMANSO	09 41S	42 04W		830 +557

TABLE 4.2 CONTINUED

PORTO NACIONAL	10 42S	48 25W	820	-60			
UTIARITI	13 02S	58 17W	1250	+276			
CUIABA	15 36S	56 06W	730	+89	390	-231	
SANTA CRUZ	15 43S	52 45W	830	+3	850	+23	
CARAVELAS	17 44S	39 15W			340	-124	
CORUMBA	19 00S	57 39W	610	+122	230	-258	
BELO HORIZONTE	19 56S	43 57W	790	-77			
TRES LAGOAS	20 47S	51 42W			630	+60	
RIO DE JANEIRO	22 54S	43 10W	370	-4			
SAO PAULO	23 33S	46 38W	700	+124			
CURITIBA	25 26S	49 16W	540	+70			
BOLIVIA							
RIBERALTA	11 00S	66 05W	500	-287	630	-157	
RURRENABAQUE	14 28S	67 35W	840	+88	550	-202	
TRINIDAD	14 45S	64 48W	610	-233	590	-253	
COCHABAMBA	17 23S	66 10W	480	+156	180	-144	
SANTA CRUZ	17 47S	63 10W	530	+63	370	-97	
CAMIRA	20 06S	63 33W	350	-131	320	-161	
YACUIBA	22 01S	63 43W	420	-125	290	-155	
PARAGUAY							
MCAL ESTIGARRIBA	22 01S	60 37W	320	0	270	-50	
ARGENTINA							
LA QUIACA	22 06S	65 36W	350	+120	250	+20	
RIVADADIA	24 10S	62 54W	230	-128			
LAS LOMITAS	24 42S	60 35W	350	+33	230	-87	
SALTA	24 51S	65 29W	600	+153	560	+113	
POSADAS	27 22S	55 58W	430	+10	310	-110	
RESISTENCIA	27 28S	58 59W	380	+37	350	+7	
CATAMARCA	28 26S	65 46W	180	-23	220	+17	
LA RIOJA	29 23S	66 49W	250	+83	200	+33	
CERES	29 53S	61 57W	320	-5	290	-35	
URAGURAY							
SALTO	31 23S	57 58W	170	-119	310	+51	
MONTEVIDEO	34 58S	56 12W	250	+16			
CHILI							
ANTOFAGASTA	23 28S	70 26W	0	0	0	0	
LA SERENA	29 55S	71 13W	0	0	0	0	
PORTUGAL							
FUNCHAL	32 38N	16 54W	500	+248	307	+144	
SAL CAPE VERDE	16 44N	22 57W	11	-5	7	-10	
GIBRALTAR							
NORTH FRONT	36 09N	05 21W	931	+551	630	+250	
MALTA							
LUQA	35 51N	14 29E	346	+125	253	+32	
CYPRUS							
NICOSIA	35 09N	33 17E	146	-46	147	-45	
GREECE							
ATHINAI	37 58N	23 43E	230	+61			
HIRAKLION	35 21N	25 08E	230	+19			

TABLE 4.2 CONTINUED

MOROCCO						
MEKNES	33 53N	05 32W	460	+211	450	+201
CASABLANCA	33 34N	07 40W	440	+235	270	+65
MARRAKECH	31 37N	08 02W	170	+80	100	+10
OUARZAZATE	30 56N	06 57W	70	+44	23	-3
AGADIR	30 23N	09 34W	300	+179	340	+219
ALGERIA						
ALGER	36 43N	03 15E	250	-59	390	+81
ORAN	35 38N	00 37W	140	-51	400	+109
LAGHOUAT	33 46N	02 56E	50	+8	110	+68
COLOMB-BECHAR	31 38N	02 15W	100	+14	25	-1
TUNESIA						
TUNIS	36 50N	10 14E			310	+123
GABES	33 53N	10 07E			140	+87
LYBIA						
ZUARA	32 55N	12 05E	145	+50	190	+95
IDRIS	32 41N	13 10E	252	+105	208	+61
MISURATA	32 25N	15 06E	130	-29	220	+61
BENINA	32 06N	20 16E	170	+14	80	-76
EL ADEM	31 51N	23 55E	32	-14	54	+8
HON	29 08N	15 57E	15	+3	1	-11
KUFRA	24 13N	23 20E	0	-T	0	-T
EGYPT						
MERSA MATRUH	31 20N	27 13E	30	-46	107	+31
HELWAN	29 52N	30 20E	7	-7	7	-7
SIWA	29 12N	25 29E	9	+2	1	-7
DAKHLA	25 29N	29 00E	0	-1	0	-1
KHARGA	25 26N	30 34E	0	-T	0	-T
ISRAEL						
LOD APT	32 00N	34 54E	290	-63	440	+89
EILAT	29 33N	34 57E	6	-10	6	-10
SAUDI ARABIA						
BAHRAIN	26 16N	50 37E	1	-49		
ADEN	12 50N	45 01E	11	-11	12	-10
SUDAN						
PORT SUDAN	19 35N	37 13E	111	+83	15	-15
TOKAR	18 26N	37 44E	75	+41	13	-22
EL OBEID	13 10N	30 14E	0	0	0	0
MALAKAL	09 33N	31 39E	0	-1	1	-1
JUBA	04 52N	31 36E	7	-21	4	-27
WAU	07 42N	28 01E	27	+23	1	-4
SENEGAL						
SAINT-LOUIS	16 01N	16 30W	T	-5	5	0
MATAM	15 38N	13 13W	0	-4	0	-4
LIBERIA						
ROBERTS FLD	06 11N	10 18W	188	+63	77	-109
IVORY COAST						
ODIENNE	09 31N	07 34W	40	+16	0	-24
ABIDJAN	05 15N	03 56W	240	+61	190	+11
TABOU	04 25N	07 22W	150	-134	100	-184
GHANA						
TAMALE	09 25N	00 53W	40	+24	0	-16
KUMASI	06 43N	01 36W	210	+87	110	-13
ACCRA	05 36N	00 10W	100	+29	70	-1
TAKORADI	04 53N	01 46W	70	-27	140	+33



TABLE 4.2 CONTINUED

DAHOMY							
KANDI	11 08N	02 56E	30	+29	0	-1	
TCHAOUROU	08 52N	02 36E	61	+32	1	-29	
SAVE	07 59N	02 26E	31	-3	10	-24	
TOGOLESE							
SOKODE	08 59N	01 08E	196	+152	0	-44	
NIGERIA							
MAIDUGURI	11 51N	13 05E	0	0	0	0	
LAGOS	06 35N	03 20E	80	-58	131	-7	
ENGU	06 28N	07 33E	70	+11	20	-37	
CONGO							
OUESSO	01 37N	16 03E	370	+141	260	0	
M POUYA	02 37S	16 13E	560	+90	380	-32	
DOLISIE	04 11S	12 40E	360	-38	350	-48	
BRAZZAVILLE	04 15S	15 14E	370	-84	540	+103	
GABON							
BITAM	02 05N	11 29E	824	+337	200	+9	
COCO-BEACH	01 00N	09 36E	1180	+264	760	-152	
LIBREVILLE	00 27N	09 25E	940	+271	600	-325	
PORT-GENTIL	00 42S	08 45E	980	+327	680	-108	
MOUILA	01 52S	11 01E	640	-70	640	-70	
CEN AFRICA							
N DELE	08 24N	20 39E	11	+1	0	-10	
BRIA	06 32N	21 59E	33	+3	18	-12	
BOUAR	05 56N	15 35E	50	+19	23	-8	
BERBERATI	04 13N	15 47E	119	+23	82	-14	
FR SOMALI							
DJIBOUTI	11 36N	43 09E	6	-27	25	-8	
CHAD							
FORT-ARCHAMBAULT	09 08N	18 23E	13	+12	0	-1	
MOUNDOU	08 37N	16 04E	6	+6	0	-1	
KENYA							
LODWAR	03 07N	35 37E	18	-5	77	+54	
NAIROBI	01 18S	36 45E	346	+168	441	+263	
UGANDA							
GULU	02 45N	32 20E			102	-9	
ENTEBBE	00 03N	32 27E			416	+137	
TANZANIA							
TABORA	05 05S	32 50E	619	+167	440	-2	
DAR ES SALAAM	06 52S	39 16E	300	+91	265	+56	
SONGEA	10 41S	35 35E	750	+42	979	+271	
ZAMBIA							
KASAMA	10 12S	31 06E	737	-15	1019	+267	
BROKEN HILL	14 27S	28 28E	889	+227	765	+100	
LIVINGSTONE	17 49S	25 49E	824	+337	448	-87	
MALAWI							
CHILEKA	15 41S	34 58E	838	+294	513	-31	

TABLE 4.2 CONTINUED

RHODESIA								
SALISBURY OBS	17	56S	31	35E	672	+198	246	-328
CHIPINGA	20	12S	32	39E	985	+355	751	+119
PORT W AFRICA								
LUANDA	08	49S	13	13E	53	-41	4	-90
MALANGE	09	33S	16	23E			500	+141
HENRIQUE	09	39S	20	24E	530	-65	620	+25
LUSO	11	47S	19	55E	730	+156	550	-24
LOBITO	12	22S	13	32E	120	+61	20	-39
NOVA LISBOA	12	48S	15	45E	630	+56		
SA DE BANDEIRA	14	56S	13	34E	540	+120	530	+110
SERPA PINTO	14	39S	13	41E	830	+326	420	-84
MOCAMEDES	15	12S	12	09E	15	-12	22	-3
MALAGASY								
DIEGO-SUAREZ	12	21S	49	18E	473	-26	565	-34
TAMATAVE	18	07S	49	24E	1191	+70	1237	+166
TANANARIVE	18	54S	47	32E	702	+66	933	+172
MANANJARY	21	12S	48	22E	894	-62	1055	+99
TULEAR	23	24S	43	44E	226	+96	102	-97
SOUTH AFRICA								
MAUN	19	59S	23	25E	380	+86		
WINDHOEK	22	34S	17	06E	300	+103	80	-117
PIETERSBURG	23	52S	29	27E	172	-81	270	+17
PRETORIA	25	45S	28	14E	220	-142	330	-32
MAFEKING	25	52S	25	38E	210	-44	180	-74
KEETMANSHOOP	26	34S	18	07E	70	0	30	-40
ISLANDS								
ST TOME IS	00	23N	06	43E			158	-106
MORONI COMORO IS	11	42S	43	14E	1028	+138	1024	+143
SERGE-FROLOW	15	53S	54	31E	560	+184	633	+257
ST DENIS	20	53S	55	31E	560	-41	820	+219
ILE EUROPA	22	21S	40	21E	278	-5	249	-34
W PAKISTAN								
MULTAN	30	12N	71	26E	22	0	30	+8
KALAT	29	02N	66	35E	10	-109	157	+38
KARACHI	24	48N	66	59E			36	+12
E PAKISTAN								
BOGRA	24	51N	89	23E	1	-33	11	-22
INDIA								
LUDHIANA	30	56N	75	52E	32	-52	15	-69
NEW DELHI	28	35N	77	12E	37	-15	28	-24
JODHPUR	26	48N	73	01E	4	-10	0	-14
ALLAHABAD	25	27N	81	44E	40	-4	13	-19
SILCHAR	24	49N	92	48E	12	-56	58	-10
DUMKA	24	16N	87	45E	5	-45	1	-50
SAGAR	23	51N	78	45E	68	+28	3	-47
DWARKA	22	22N	69	05E	0	-6	0	-6
CALCUTTA	22	32N	88	20E	0	-40	10	-30
CUTTACK	20	48N	85	56E	0	-42	31	-11
BOMBAY	18	54N	72	49E	57	+52	50	+45
VISHAKHAPATAM	17	43N	81	14E	6	-33	5	-34
MADRAS	13	00N	80	11E			118	-70
BANGALORE	12	58N	77	35E	109	+80	15	-14
PAMBAN	09	16N	79	18E	320	+39	233	-48

TABLE 4.2 CONTINUED

CEYLON								
MANNAR	08	59N	79	55E	460	+125	410	+75
COLOMBO	06	54N	79	52E	370	0	520	+150
HAMBANTOTA	06	87N	81	08E	390	+102	410	+132
JAPAN								
TOKYO	35	41N	139	46E	84	-98	243	+60
YONAGO	35	26N	133	21E	540	+83	410	-37
NAGOYA	35	10N	136	58E	94	-76	184	+14
FUKUOKA	33	35N	130	23E	277	+47	280	+50
NAGASAKI	32	44N	129	53E	220	-20	248	+8
TORISHIMA	30	29N	140	18E	387	+46	282	-69
NAZE	28	23N	129	30E	321	-186	693	+186
MAWASHI	26	14N	127	41E	269	-155	369	55
MIYAKOJIMA	24	47N	125	17E	234	-183	592	+175
SOUTHEAST ASIA								
TAIPEI	25	02N	121	31E	108	-207	423	+108
HONG KONG	22	18N	114	10E	11	-86	113	+6
BANGKOK	13	44N	100	30E			14	-31
LUANG PRABANG	19	53N	102	08E	10	-98		
VIENTIANE	17	57N	102	34E	3	-63		
PATTLE	16	33N	111	37E	25	-75	100	0
SIAGON	10	49N	106	40E	56	0	35	-21
RANGOON	16	46N	96	10E			70	+54
VICTORIA POINT	09	58N	98	35E			110	+36
KOTA BHARU	06	10N	102	17E	650	-180	560	-250
KUALA LUMPUR	03	07N	101	42E	320	-260	830	+250
SINGAPORE	01	21N	103	54E	780	+25	1050	+295
DJAKARTA	06	11S	106	50E	1429	+569	360	-409
DILL	08	35S	125	34E			287	-192
AUSTRALIA								
THURSDAY IS	10	35S	142	13E	680	-336	950	+55
COCOS IS	12	05S	96	53E	380	+52	222	-96
DARWIN	12	26S	130	52E	830	-113	670	-242
DALY WATERS	16	16S	133	23E	350	-53	200	-203
BROOME	17	57S	122	13E	410	+7	450	+47
HALLS CREEK	18	160	127	37E			170	-152
TOWNSVILLE	19	15S	146	46E	630	+5	720	-8
CLONCURRY	20	40S	140	30E	220	-119	304	-6
NULLAGINE	21	54S	120	06E	400	+110	46	-144
ROCKHAMPTON	23	23S	150	29E	330	-71	210	-191
LONGREACH	23	26S	144	15E	190	+6	190	+6
ALICE SPRINGS	23	480	133	03E	13	-104	20	-80
PHILIPPINES								
BASCO	20	27N	121	58E	339	-335	612	-62
APARRI	18	22N	121	38E	413	-58	477	-14
MANILA	14	31N	121	00E	3	-78	132	+51
ILOILO	10	42N	122	34E	34	-178	490	+278
ZAMBOANGA	06	54N	122	04E	350	+54	193	-3

TABLE 4.2 CONTINUED

PACIFIC ISLANDS

WAKE	19	17N	166	39E	84	-25	82	-27
GUAM	13	33N	144	50E	810	+448	566	+204
ENIWETOK	11	21N	162	21E	250	+106	255	+104
YAP	09	31N	138	08E	978	+392	482	-94
KWAJALEIN	08	43N	167	44E	438	+63	459	+84
TRUK	07	28N	151	51E	753	+44	566	-153
MAJURO	07	05N	171	23E	983	+307	430	-116
PONAPE	06	58N	158	13E	1294	+300	824	-170
LIHUE	21	59N	159	21W	378	-29	284	-123
HILO	19	44N	155	04W	131	-884	855	-106
JOHNSON	16	44N	169	31W	32	-182	81	-133
RABAUL	04	13S	152	11E	300	-378	640	-138
LAUTHALA BAY	18	09S	178	27E	810	-115	1240	+210
KOUMAC	20	32S	164	15E	520	+126	276	-218
CANTON	02	46S	171	43W	19	-166	654	+469
ATOUNA	09	48S	139	02W	210	-38	270	+42
APIA	13	48S	171	48W	887	-286	911	-252
TAKAROA	14	30S	145	05W	540	-90	390	-240
BORA BORA	16	31S	151	56W			730	-12
MOPELIA	16	55S	154	00W	390	-258	640	-8
TAHITI	17	32S	149	35W	710	-205	710	-205
RIKITEA	23	07S	134	57W	600	-45	360	-285

TABLE 5.1

Mean Meridional Velocity (m/sec) And Momentum Transport  
( $\text{m}^2/\text{sec}^2$ ) By Transient Eddies For 200 mb.

	Dec 62-Feb 63		Dec 63-Feb 64	
	$[\bar{v}]$	$[\overline{u'v'}]$	$[\bar{v}]$	$[\overline{u'v'}]$
25N	-1.16	20.56	1.01	25.17
20N	0.60	8.75	1.12	15.36
10N	1.90	-6.36	1.71	-15.50
EQ	1.41	-7.92	1.43	-10.25
10S	0.22	-9.89	-0.48	-9.75

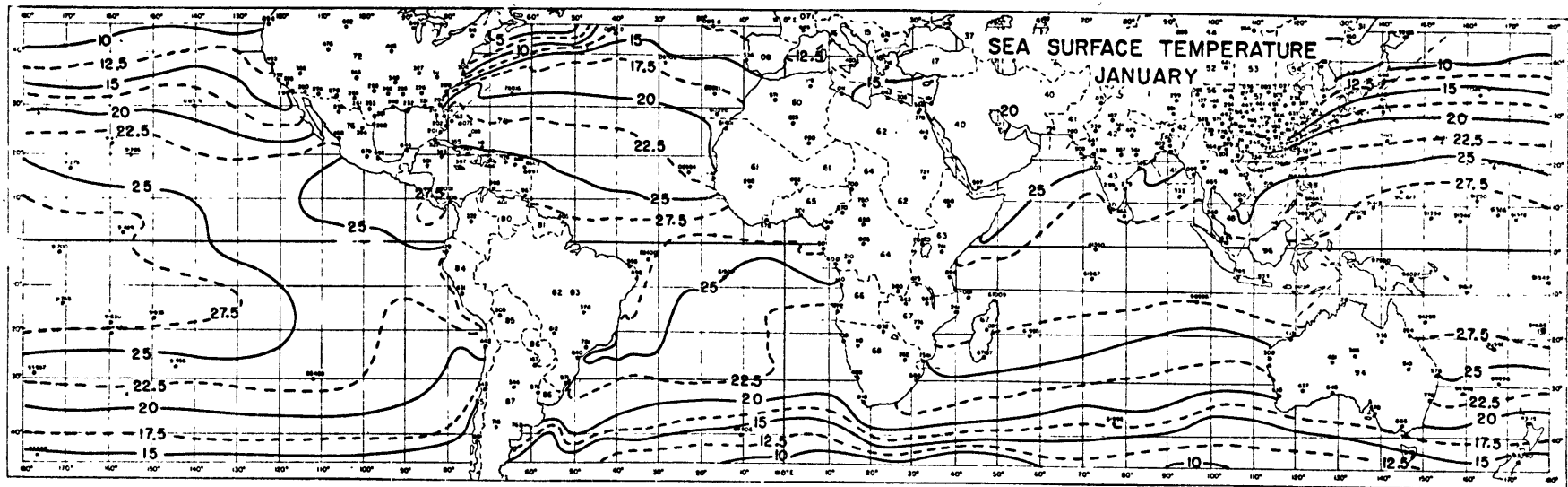


Figure 1.1: Mean sea-surface temperature for January (°C)  
(Hydrographic Office, U.S. Navy, 1944)

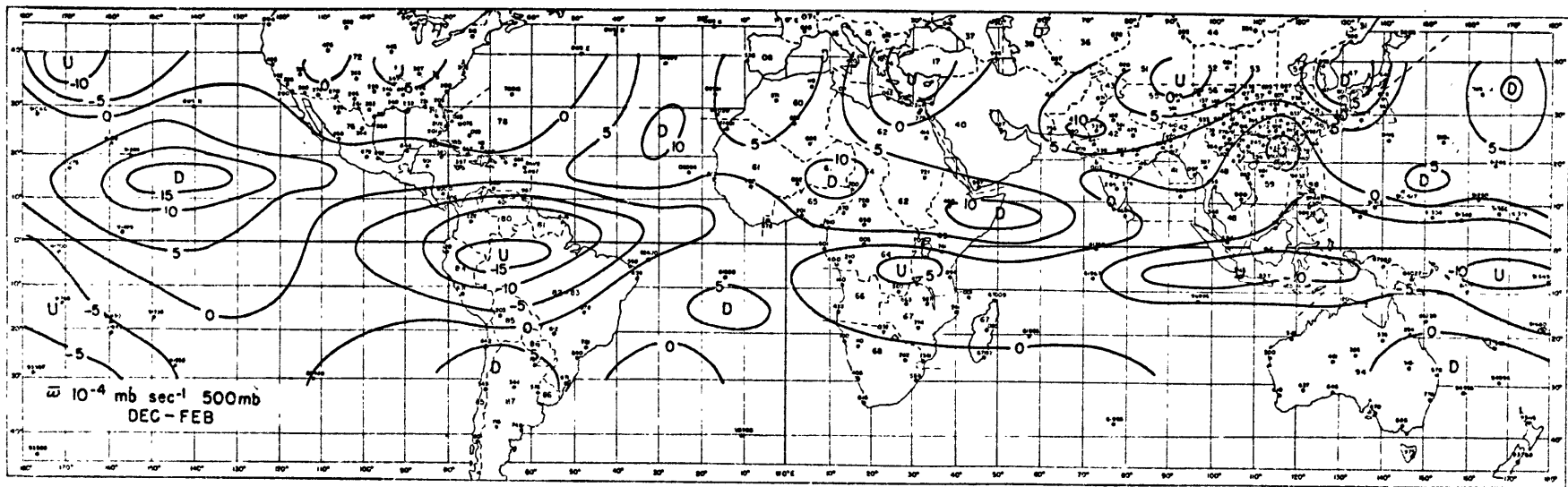


Figure 3.1: Mean vertical velocity at 500 mb for December-February.  
 Units:  $10^{-4}$  mb/sec.

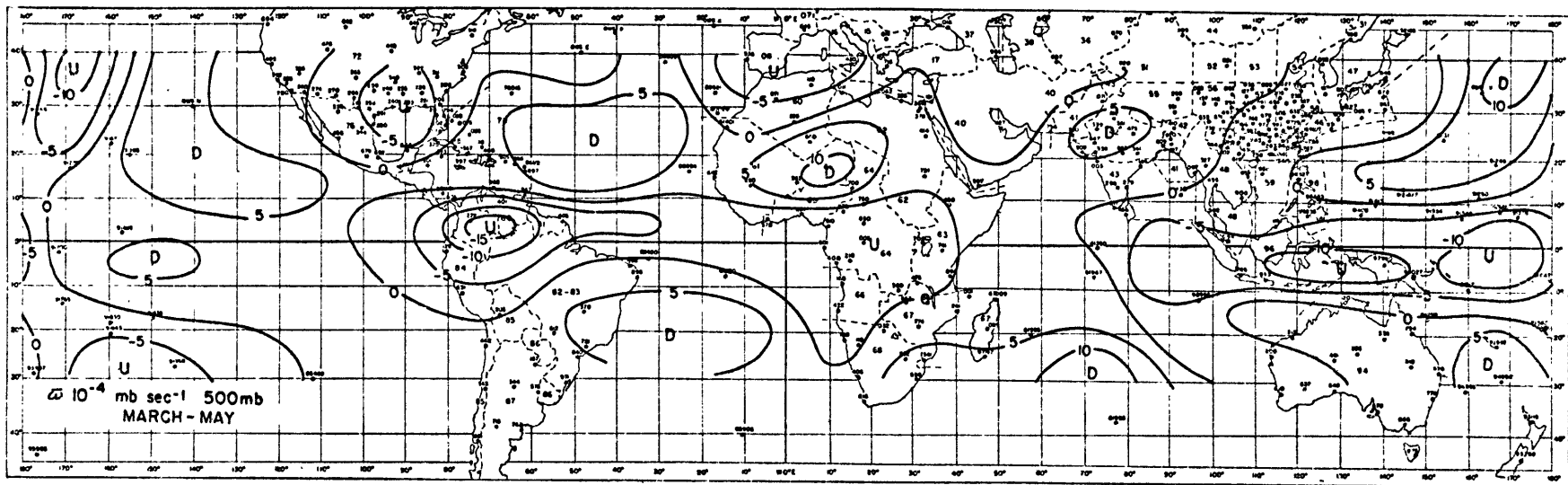


Figure 3.2: Mean vertical velocity at 500 mb for March-May.  
 Units:  $10^{-4}$  mb/sec.



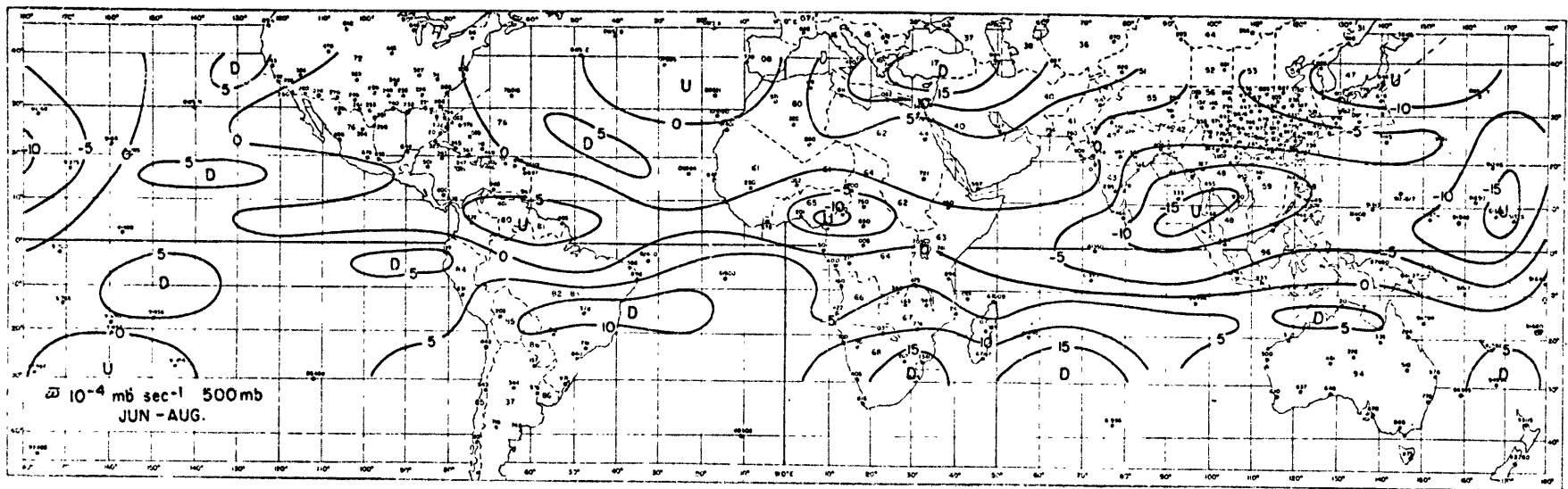


Figure 3.3: Mean vertical velocity at 500 mb for June-August.  
 Units:  $10^{-4}$  mb/sec.

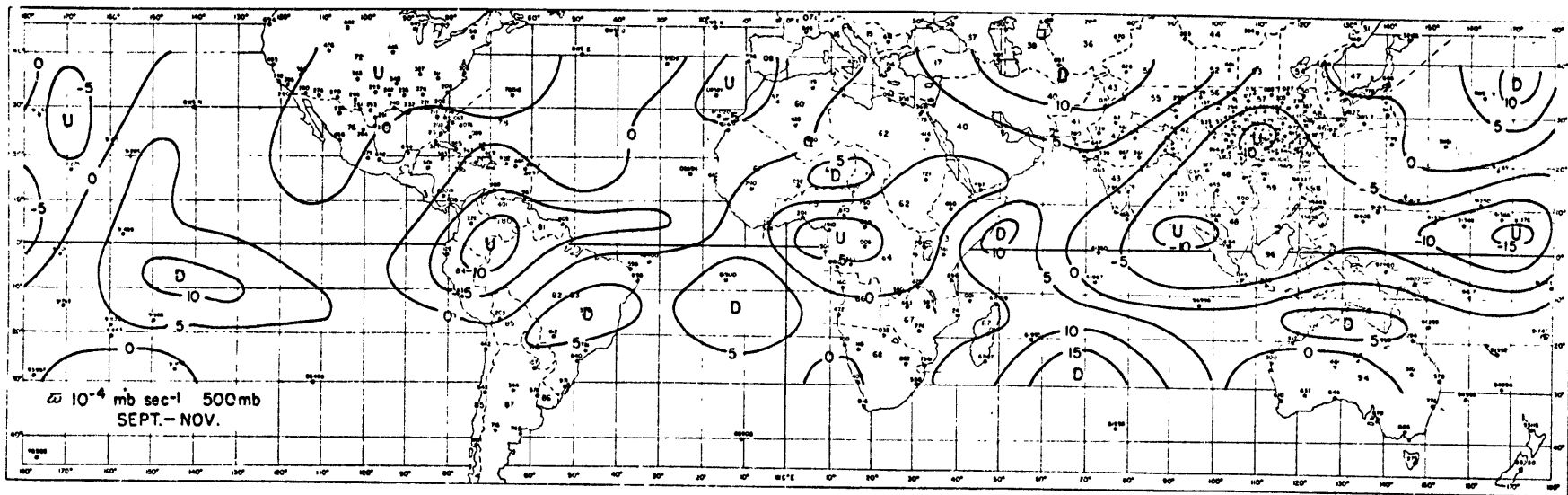


Figure 3.4: Mean vertical velocity at 500 mb for September–November.  
 Units:  $10^{-4}$  mb/sec.

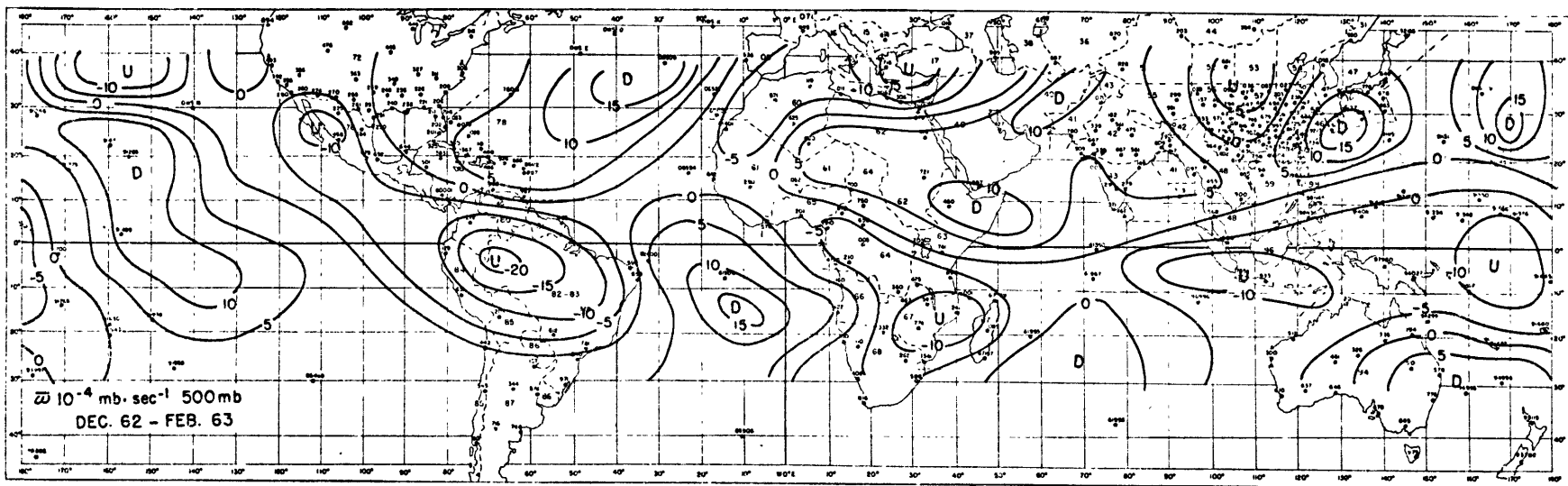


Figure 4.1: Mean vertical velocity at 500 mb for December 1962-February 1963.  
 Units:  $10^{-4}$  mb/sec.

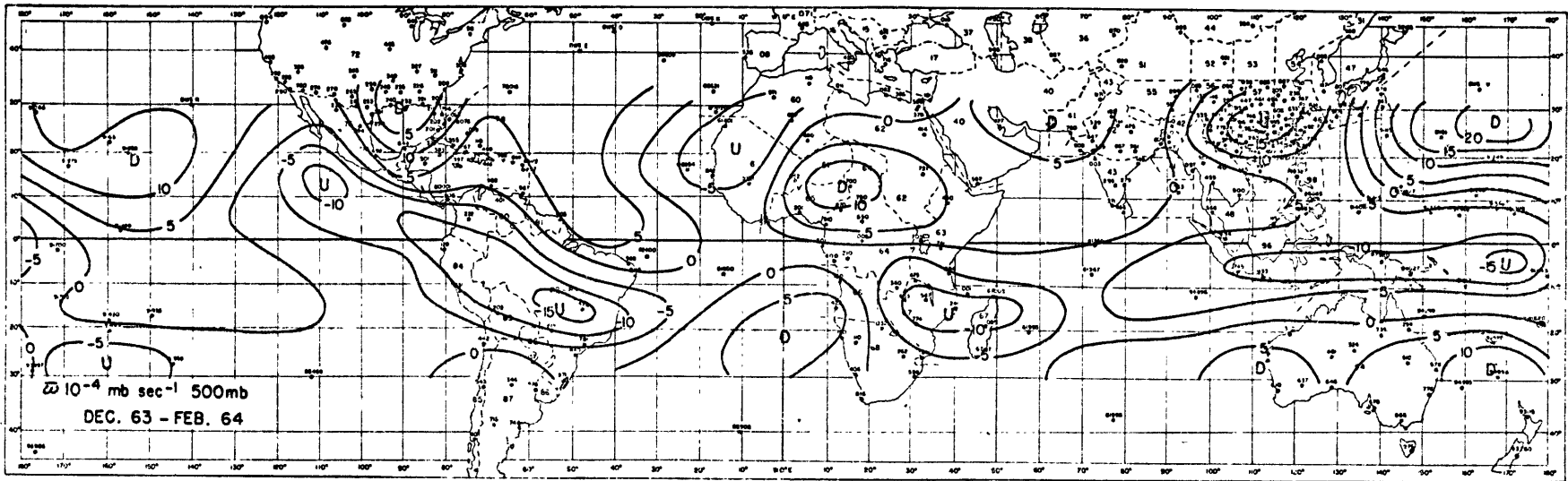


Figure 4.2: Mean vertical velocity at 500 mb for December 1963–February 1964.  
 Units:  $10^{-4}$  mb/sec.

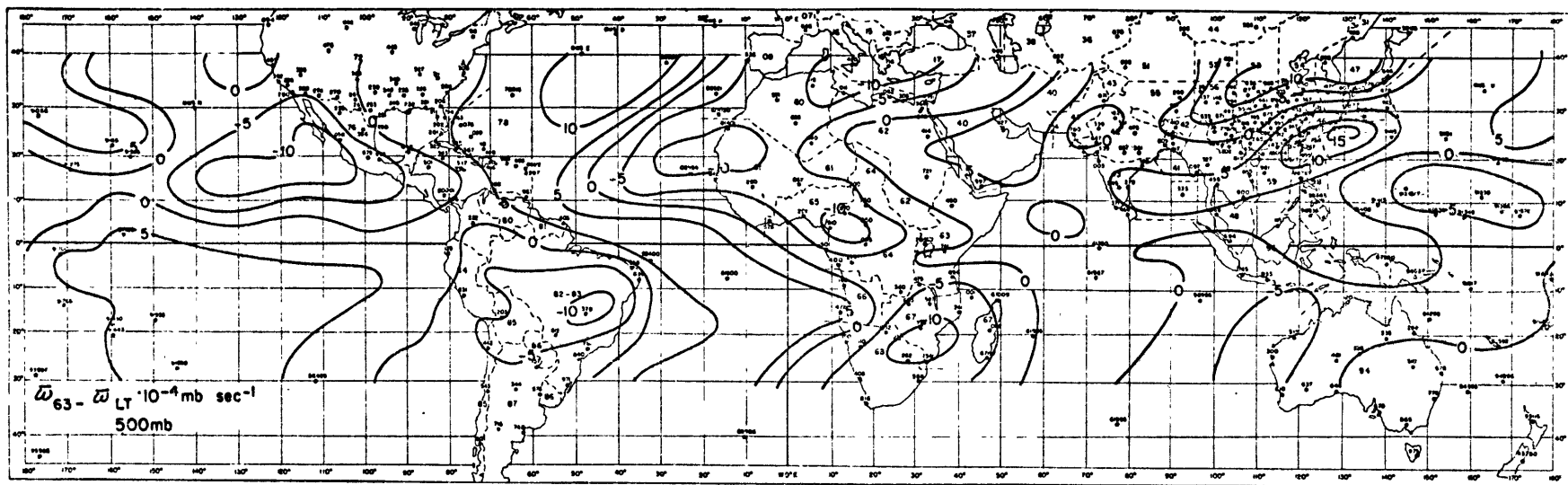


Figure 4.3: Deviation of mean vertical velocity at 500 mb for December 1962-February 1963 from the long term mean for December-February. Units:  $10^{-4}$  mb/sec.

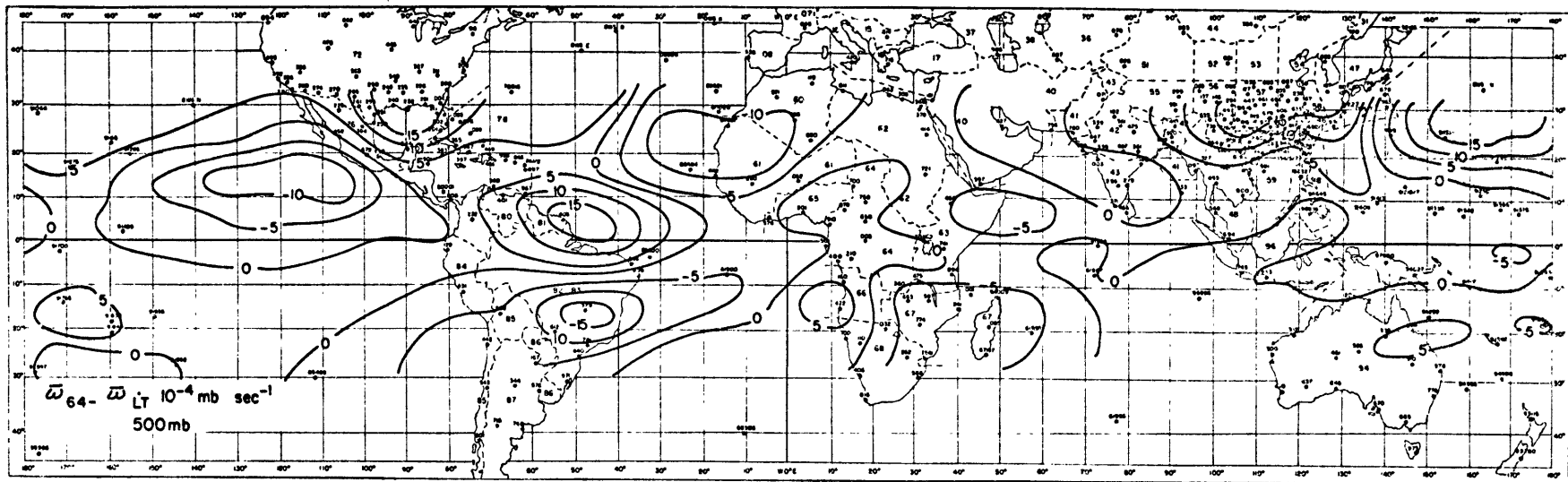


Figure 4.4: Deviation of mean vertical velocity at 500 mb for December 1963-February 1964 from the long term mean for December-February. Units:  $10^{-4}$  mb/sec.

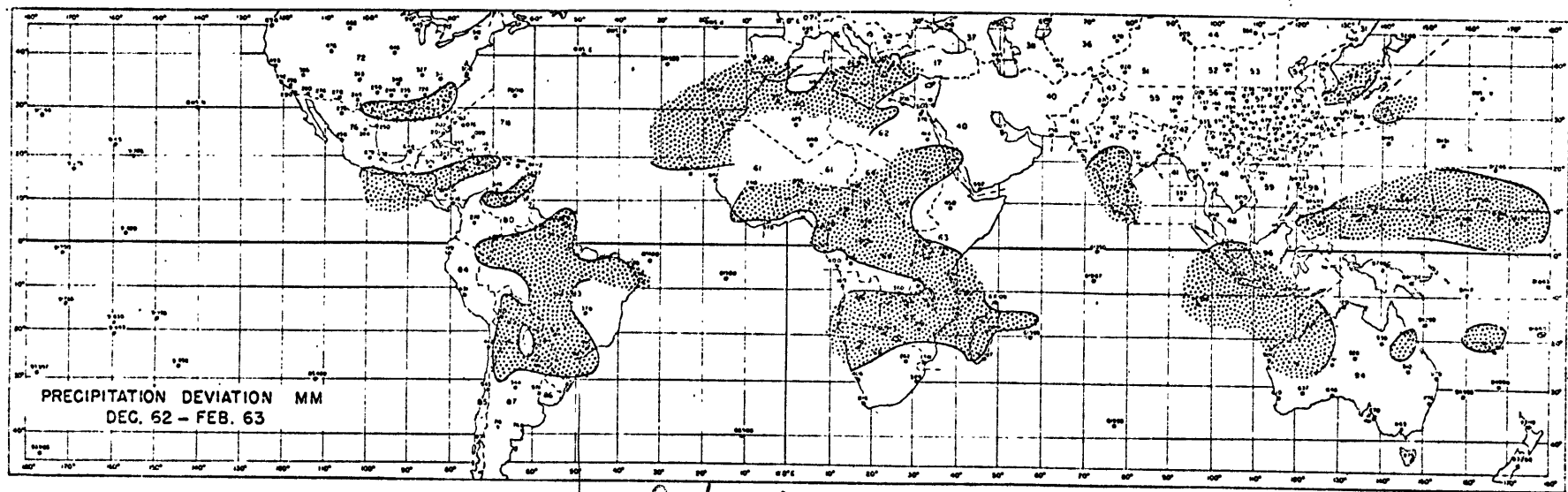


Figure 4.5: Total deviation of precipitation for December 1962-February 1963 from the 30 year mean. Units: mm.

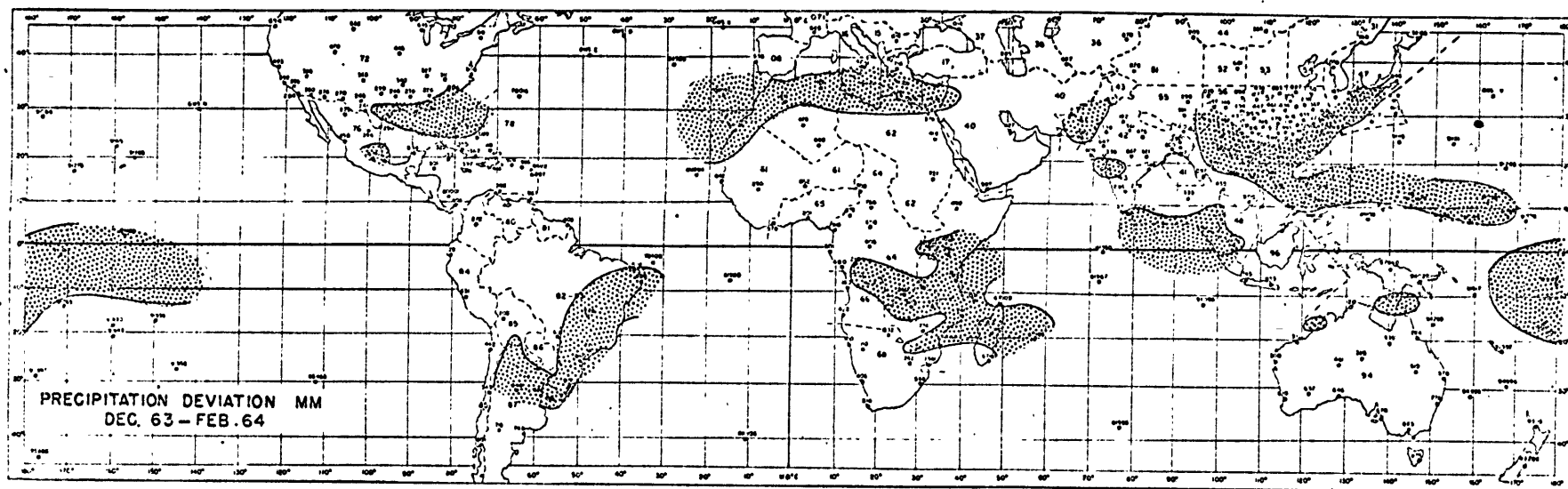


Figure 4.6: Total deviation of precipitation for December 1963-February 1964 from the 30 year mean. Units: mm.



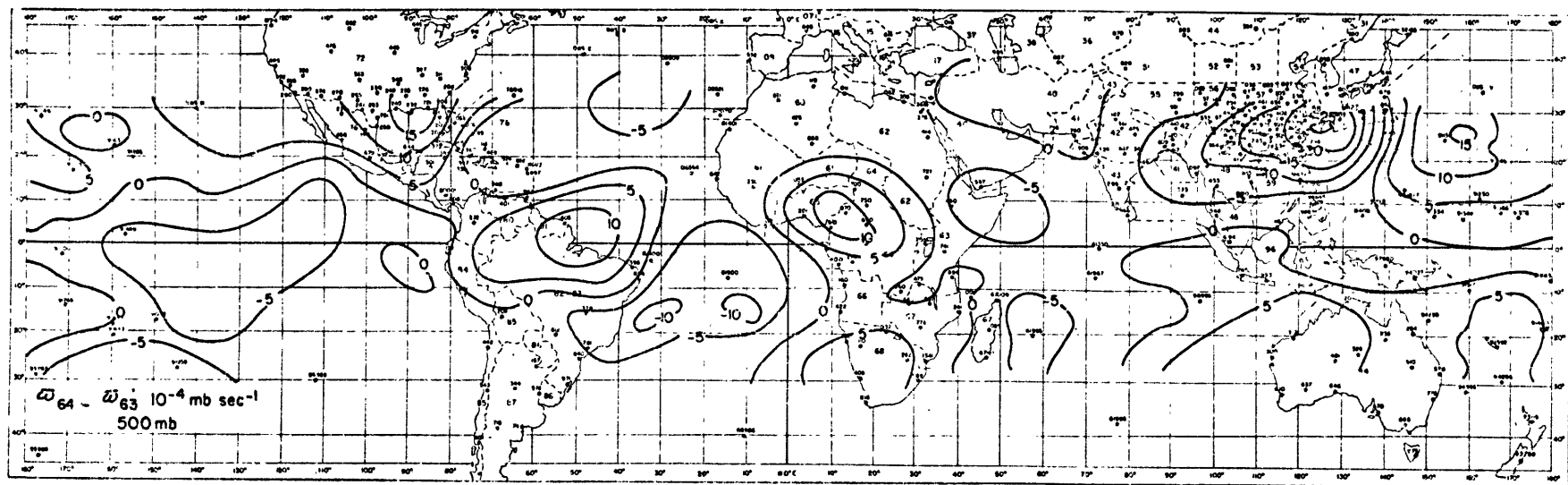


Figure 5.1: Change in mean vertical velocity from December 1962-February 1963 to December 1963-February 1964 at 500 mb. Units:  $10^{-4}$  mb/sec.